



Published in final edited form as:

*Macromolecules*. 2009 April 28; 42(8): 3152–3161. doi:10.1021/ma802250c.

## Electrophoretic Behavior of Anionic Triazine and PAMAM Dendrimers: Methods for Improving Resolution and Assessing Purity Using Capillary Electrophoresis

Sanjiv Lalwani<sup>\*,†</sup>, Vincent J. Venditto<sup>†</sup>, Abdellatif Chouai<sup>†</sup>, Gregory E. Rivera<sup>†</sup>, Sunil Shaunak<sup>‡</sup>, and Eric E. Simanek<sup>†</sup>

<sup>†</sup>Department of Chemistry, Texas A&M University, College Station, Texas 77843

<sup>‡</sup>Faculty of Medicine, Imperial College London, Hammersmith Hospital, Ducane Road, London, W12 0NN, U.K

### Abstract

The synthesis and characterization of second- and third-generation triazine dendrimers bearing carboxylic acid groups on the periphery are reported. These materials were synthesized by exhaustive succinylation of amine-terminated dendrimers. <sup>1</sup>H and <sup>13</sup>C NMR spectra are consistent with the desired products, but these techniques are limited by degeneracy in signals. MALDI-TOF mass spectrometry confirms the presence of the desired material. These materials display pH-dependent solubility in water. Capillary electrophoresis proves to be valuable in multiple elements of this work, and general protocols emerge that appear to be useful for the characterization of lower-generation anionic dendrimers. Specifically, capillary electrophoresis provides a convenient method for monitoring the removal of excess succinic anhydride/succinic acid and offers additional clues to the chemical nature of the impurities in these samples. Optimization of the background electrolyte and instrumental parameters allows for the assessment of the purity of these triazine targets as well as comparison with two sets of commercially available anionic poly(amidoamine) (PAMAM) dendrimers. Corroborative information from the different orthogonal analytical techniques employed supports the hypothesis that triazine dendrimers exist as very narrowly disperse mixtures of macromolecules approaching, in some cases, single chemical entities.

### Introduction

Polymeric materials are notoriously difficult to characterize unambiguously, and significant energy has been invested in the evaluation of purity of these materials and the assignment and quantification of impurities.<sup>1–6</sup> Even “well-defined” polymers such as dendrimers yield degenerate NMR signals<sup>1,2</sup> and suspect spectra derived from mass spectrometry.<sup>4</sup> Confidence in purity is usually derived from a collection of corroborative methods.<sup>5,6</sup> The recent kilogram-scale synthesis of a triazine dendrimer<sup>7</sup> provided materials judged conservatively as being approximately 93% pure solely on the basis of reversed-phase HPLC analysis of the penultimate, BOC-protected intermediate. Chemical clues to the

© 2009 American Chemical Society

\*Corresponding author. E-mail: simanek@tamu.edu.

**Supporting Information Available:** <sup>1</sup>H NMR, <sup>13</sup>C NMR, and MALDI-TOF-MS of second generation succinate triazine dendrimer; <sup>1</sup>H NMR, <sup>13</sup>C NMR, and MALDI-TOF-MS, and electropherograms under varying ionic strength conditions of generation three succinate triazine dendrimer; and MALDI-TOF-MS of DAB-PAMAM-S and DAB-PAMAM-C dendrimers and lot numbers for PAMAM dendrimers used. This information is available free of charge via the Internet at <http://pubs.acs.org>.

nature of the impurities were not available: MALDI-TOF-MS analysis revealed a single species, retention times on HPLC columns were not predictable across a range of intermediates, and the NMR spectra were broad. Scalable manufacturing for value-added uses (i.e., drug delivery, diagnostic imaging, etc.) requires that major challenges in the areas of quality control be addressed including batch-to-batch reproducibility in synthesis and assessment of purity.

Dendrimers have been subjected to a range of analytical assessments including numerous light-scattering, spectroscopic, electrochemical, and separation techniques.<sup>5</sup> Elemental analysis of dendrimers, in general, is problematic; the polymeric nature of these macromolecules and their inherent ability to act as hosts for small molecule guests, including molecules of solvent, have made these data difficult to obtain. Structural information available through spectroscopic techniques including nuclear magnetic resonance (NMR) spectroscopy is often limited by signal degeneracy as well as broad lines due to multiple conformational states that are sampled on the NMR time scale. Although mass spectrometry (MS) provides evidence of existence and is highly sensitive, it is not reliably quantitative because of variations in ionization efficiencies. Signals from minor components can be enhanced or suppressed because of differences in composition and instrumental parameters including choice of matrix in MALDI experiments. High-performance liquid chromatography (HPLC) is an essential tool, although its usefulness is limited when dealing with species with slight structural differences but markedly similar composition (i.e., a dendrimer bearing 11 versus 12 succinic acid groups). New methodologies continue to be advanced, including recently, a UPLC technique.<sup>8</sup> Although not commonly employed by synthetic organic chemists, data derived from capillary electrophoresis (CE) enriches the assessment of purity by contributing information orthogonal to conventional methods.

CE is an important technique for assessing a range of different water-soluble analytes including the dendrimers described here. Specifically, the expected impurities will oftentimes differ in charge state from the desired product. For example, in the case of the triazine dendrimers reported in this manuscript, a failed succinylation of a primary amine group would shift the expected residue charge by up to +2 units depending on the pH. In CE, separation results from the differential rate of migration of charged species under an applied electric field in an electrically conducting medium (termed the background electrolyte, BGE, typically a buffer solution) contained in a fused silica capillary tubing (typically of 25–100  $\mu\text{m}$  internal diameter). Because the rate of migration is directly proportional to the charge and inversely proportional to the hydrodynamic radius of the species, resolution in CE is based on the difference in the charge-to-size ratios of the analytes. The relatively high separation efficiency attainable in CE, which is typically higher than most chromatographic separations, permits the separation of analytes that are structurally very similar (e.g., protein charge ladders, DNA fragments, enantiomers, etc.) as well as synthetic polymers.<sup>9</sup>

Although the use of CE for analysis of dendrimers has been reported, most analyses focused on the separation of different generations of dendrimers and not on accurate purity assessments and physicochemical characterizations within a single generation. Huang et al. presented the results of an elegant and thorough study on the effect of pH and ionic strength on the mobility of second- to fifth-generation cascade polymers and identified the effects of counterion binding on charged spheres.<sup>10</sup> Seyrek et al. reported a previously unnoticed electric-field dependency on the mobility of carboxylate second- to fifth-generation dendrimers.<sup>11</sup> Shi et al. used CE, among other techniques to characterize generations two to seven succinamic acid derivatives of ethylenediamine-core PAMAM dendrimers.<sup>12</sup>

Using CE to assess purity, however, introduces additional challenges: the certainty with which an observed single peak in a CE trace implies monodispersity in the sample is highly dependent on the use of a method optimized to provide maximum resolution. Accordingly, such studies require evaluation of the electrophoretic behavior of dendrimers by careful manipulation of multiple, interdependent, operational parameters, such as, capillary length, BGE composition, and so on. An early study by Brothers et al. hints at the potential for use of CE in the assessment of dendrimer purity wherein the hydrolysis of terminal carboxylate methyl ester groups of generation 1.5 and generation 3.5 dendrimers were described.<sup>13</sup> Our work complements strategies recently reported by Desai et al., who described the use of capillaries coated with polyvinyl alcohol for similar purposes.<sup>14</sup>

Here we report the synthesis and characterization of second- and third-generation triazine dendrimers (Chart 1). CE proves to be valuable in quantitatively monitoring the removal of excess reagent and side-product concentrations: these materials are largely invisible to <sup>1</sup>H NMR spectroscopy and MALDI-TOF-MS. After extensive method development, CE allows for an assessment of the purity of the triazine dendrimers. Comparison of these data with those derived from two classes of commercially available anionic PAMAM dendrimers (Chart 1) allows us to impose limits of confidence and describe needs for further theoretical and experimental efforts in this area.

## Experimental Section

### Materials

All chemicals for the preparation of the BGEs and all reagents and solvents needed in the succinylation of triazine dendrimers were purchased from Aldrich Chemical Co. (Milwaukee, WI) and used as received. Commercial diaminobutane—core PAMAM carboxylate dendrimers (DAB-PAMAM-C) and diaminobutane—core PAMAM succinate dendrimers (DAB-PAMAM-S) were also purchased from Aldrich Chemical Co. Second- and third-generation, amine-terminated triazine dendrimers were synthesized in our laboratory, as previously reported.<sup>15</sup>

### Capillary Electrophoresis

All CE separations were obtained using a P/ACE MDQ capillary electrophoresis system with a photodiode array detector (Beckman-Coulter, Fullerton, CA). Bare fused silica capillaries (Polymicro Technologies, Phoenix, AZ) used had an internal diameter of 50  $\mu$ m and typical lengths as follows: total length of the capillary,  $L_t$ , 30.6 cm; length of the capillary from injection point to the detection window,  $L_d$ , 20.7 cm. Lengths  $L_t$  and  $L_d$  varied from cartridge-to-cartridge by  $\pm 0.5$  cm. Conditions used for all CE experiments were as follows: applied potential, 30 kV; detection wavelength, 214 nm; temperature, 25  $^{\circ}$ C. For purposes of discussion, representative electropherograms are shown to demonstrate the individual principles.

The different BGEs used were made by first preparing a solution of the buffering species of the desired concentration, followed by titration to the desired pH using the titrant in the pure form (as solid or liquid). Further details on the selection of BGE components and preparation are provided in the Results and Discussion section. Solutions of 0.2 to 0.5% dimethyl sulfoxide (DMSO) in water were used as the neutral marker. Initial accurate estimates of analyte effective mobility were obtained using the pressure-mediated CE (PreMCE) protocol,<sup>16</sup> followed by conventional CE runs. The sequence for the conventional CE method was as follows: 0.5 min rinse of the capillary with the BGE at 20 psi; 3 s injection of the neutral marker solution at 0.5 psi; 3 s injection of the sample solution at 0.5 psi, either from the same or the opposite end depending on the polarity; and last, electrophoresis under either positive-to-negative or negative-to-positive polarity, as

applicable, with simultaneous detection. When desired, the time scale on the electropherograms was converted to an effective mobility scale using the Microsoft Excel software package.

### Nuclear Magnetic Resonance and Mass Spectrometry Characterization

$^1\text{H}$  and  $^{13}\text{C}$  NMR were obtained using a Mercury 300 instrument in  $\text{D}_2\text{O}$ . Chemical shifts are reported in parts per million on the  $\delta$  scale relative to solvent. MALDI-TOF mass spectra were performed on an ABI Voyager-DE STR mass spectrometer operating in reflected mode using 2,4,6-trihydroxyacetophenone (THAP) as matrix.

### Synthesis of Second-Generation Succinate Triazine Dendrimer

Succinic anhydride (11.77g, 0.12 mol) was added to a stirring solution of G2 dendrimer (2.87g, 0.97 mmol) dissolved in 150 mL of water:acetonitrile:tetrahydrofuran (2:2:1), followed by diisopropylethylamine (20 mL, 0.12 mol). The reaction was stirred at room temperature for 48 h and was then concentrated in vacuo to afford a thick white gel. The product was then alkalinized to pH 11 using 5% sodium hydroxide and diluted with water. The solution was then added to an Amicon ultrafiltration stirred cell and passed through a YM3 membrane under nitrogen pressure. The retentate was collected and concentrated to yield a white solid (2.94 g, 72.7%).  $^1\text{H}$  NMR ( $\text{D}_2\text{O}, \delta$ ): 4.00-2.75 (br m, 132H), 2.41 (br s, 48H), 2.00-0.75 (br m, 90H).  $^{13}\text{C}$  NMR ( $\text{D}_2\text{O}, \delta$ ): 180.7, 175.1, 165.3, 164.8, 164.2, 44.0, 37.0, 33.1, 32.3, 27.0, 25.5. MS (MALDI-TOF): calcd for  $\text{C}_{189}\text{H}_{300}\text{N}_{72}\text{O}_{36}$ , 4154.39; found, 4155.86 ( $\text{M} + \text{H}$ ) $^+$ .

### Synthesis of Third-Generation Succinate Triazine Dendrimer

Succinic anhydride (14.1 mg, 0.14 mmol) was added to a stirring solution of G3 dendrimer (21.2 mg, 0.003 mmol) dissolved in 1.1 mL of water:acetonitrile:tetrahydrofuran (5:5:1), followed by diisopropylethylamine (0.20 mL, 1.20 mmol). The reaction was stirred at room temperature for 48 h and was then concentrated in vacuo to afford a thick off-white gel. The product was then alkalinized to pH 11 using 5% sodium hydroxide and diluted with water. The solution was added to an Amicon ultrafiltration stirred cell and passed through a YM3 membrane using nitrogen. The retentate was then collected and concentrated to yield a white solid (2.94 g, 73%).  $^1\text{H}$  NMR ( $\text{D}_2\text{O}, \delta$ ): 4.00-2.75 (br m, 180H), 2.41 (br s, 96H), 2.00-0.50 (br m, 210H).  $^{13}\text{C}$  NMR ( $\text{D}_2\text{O}, \delta$ ): 181.6, 176.3, 166.7, 165.9, 165.3, 45.2, 38.3, 34.3, 33.6, 29.0, 28.4, 26.1. MS (MALDI-TOF): calcd for  $\text{C}_{405}\text{H}_{648}\text{N}_{156}\text{O}_{72}$ , 8849.20; found, 8859.50 ( $\text{M} + \text{H}$ ) $^+$ .

## Results and Discussion

The Results and Discussion portion of this paper is divided into four sections. The first section describes the synthesis of second- and third-generation succinylated triazine dendrimers including the use of indirect-UV detection CE to monitor the removal of succinic acid by ultrafiltration. The second section describes the process of selecting an appropriate BGE for the analysis of anionic dendrimers by CE. Optimization of resolution by manipulation of the operational parameter  $\beta$  is described in section three. Further attempts to optimize resolution, on the basis of the operational parameter  $\alpha$ , by changing the ionic strength and pH are described in section four. Throughout the discussion, results obtained from the analysis of triazine dendrimers are compared with those obtained from the analysis of commercially available PAMAM dendrimers with a similar number of carboxylic acid groups.<sup>17,18</sup> Batch-to-batch variability leads us to report batch numbers for PAMAM lots in the Supporting Information and caution about global conclusions based on the evaluation of a single batch of these materials.

## Synthesis and Characterization of Anionic Triazine Dendrimers

The synthesis of the amine-terminated triazine dendrimers has been reported.<sup>15</sup> It relies on a divergent, iterative synthetic scheme<sup>19</sup> wherein the triamine core is reacted with a dichlorotriazine bearing two BOC-protected amines, the resulting monochlorotriazine groups are capped with piperidine, and the BOC groups are removed with acid (Scheme 1). Exhaustive succinylation is accomplished using a 10:1 ratio of succinic acid anhydride to amine. Excess reagent and succinic acid were removed by first titrating the reaction mixture to pH 11 using 5% sodium hydroxide solution to saponify the anhydride, followed by ultrafiltration. These materials gave satisfactory <sup>1</sup>H and <sup>13</sup>C NMR and appeared to be single high-molecular-weight species by MALDI-TOF MS.

## Quantifying the Excess Succinic Acid Using Capillary Electrophoresis

Detecting trace amounts of succinic acid is problematic: NMR methods suffer from both signal-to-noise limitations and broad traces. Because succinic acid does not have a strong UV absorbance at 214 nm, indirect-UV detection can be accomplished using CE. A 20 mM BisTris/5 mM phthalic acid buffer (pH 6.4, *I* = 10 mM) was used as the BGE, and analysis was done in negative-to-positive polarity (i.e., negatively charged electrode at the injection end of the capillary, also the end farther away from the detector, and positively charged electrode at the outlet end of the capillary, also the end closer to the detector). A calibration curve was obtained by analyzing standard solutions of succinic acid prepared from 0.31 to 2.5 mg/mL prepared by serial dilution. Figure 1 shows the electropherograms for solutions of succinic acid used to obtain the calibration curve.

Solids obtained from the reaction mixture, after being subjected to purification cycles via ultrafiltration, were dissolved in water at a concentration of 25 mg/mL. The solution was analyzed using the indirect-UV detection CE method, and the concentration corresponding to the peak area for the succinic acid signal was determined. Representative traces corresponding to the amount of succinic acid in the second-generation triazine dendrimer reaction mixture are shown as an inset in Figure 1. After the first purification cycle, the concentration of succinic acid was 0.5 mg/mL, corresponding to the removal of ~97% of the excess succinic acid from the mixture. The concentration of succinic acid after the second cycle of ultrafiltration was 0.15 mg/mL resulting in a material that was >99 wt % dendrimer.

## Selection of an Appropriate Background Electrolyte

Our choice of an appropriate BGE for the analysis of dendrimers with weakly acidic or weakly basic functional groups was based on five criteria. First, the pH was selected such that the analytes are sufficiently charged to exhibit significant electrophoretic mobility. Second, the concentration was selected such that the BGE exhibits significant buffering capacity. Third, the BGE components were selected such that optimum buffering capacity is obtained at the desired pH with minimal conductivity to minimize the resulting current and as a consequence, Joule heating. Fourth, the closest possible match is obtained between the electrophoretic mobilities of the analytes and the BGE coion to minimize band broadening due to electromigration dispersion (EMD). Lastly, interference from “system peaks” (also known as eigenpeaks) must be avoided.

Because the carboxylated dendrimers of interest bear a significant negative charge at and above pH 9, a borate/lithium buffer was chosen: 100 mM buffer (100 mM solution of boric acid titrated with lithium hydroxide) with a pH of 9.1 (50 mM ionic strength). Unlike every other buffer system where the pH of the solution is dependent solely on the ratio of the concentrations of the weak acid and its conjugate base, borate buffers are unique because of secondary chemical equilibria involving the formation of polyborates; the pH of the solution is dependent on both the ratio of boric acid and its conjugate base as well as the actual

concentrations of the two species. However, at a boric acid-to-borate ratio of 1:1, the pH of a borate buffer solution (pH of ~9.1) becomes essentially independent of the actual concentration of the two species. This becomes a crucial function when the effect of ionic strength on the electrophoretic behavior of selected dendrimers, under constant pH conditions, is explored later in this work. Estimation of the effective mobility values for the anionic dendrimers at pH 9.1 using the PreMCE method<sup>16</sup> combined with the use of the Peakmaster 5.1 software package<sup>20–22</sup> indicated that the borate/lithium buffer was an ideal BGE due to the similar effective mobilities for borate and the dendrimers and the absence of interfering “system peaks”.

### Optimization of Resolution

**Theory**—Optimization of resolution in CE is guided by the parameters described by Rawjee and Vigh<sup>23</sup> in the following extended resolution equation

$$R_s = \left(\frac{El}{8}\right)^{1/2} \frac{\text{abs}(\alpha - 1)(\alpha + \beta)^{1/2}(1 + \beta)^{1/2}}{(\alpha + \beta)^{3/2}D_2^{1/2} + (1 + \beta)^{3/2}D_1^{1/2}} \mu_2^{1/2} \quad (1)$$

where  $E$  is the field strength during electrophoresis;  $l$  is the length of the capillary;  $\alpha$  is the mobility ratio, or the selectivity, which is defined as the ratio of the mobilities of the two analytes being separated;  $\beta$  is the transport coefficient or the “normalized electroosmotic flow (eof)”, which is defined as the ratio of the mobility due to eof and the mobility of the less mobile analyte; and  $D_1$  and  $D_2$  are the diffusion coefficients for the more mobile analyte (1) and the less mobile analyte (2).

Accordingly, high field strengths (i.e., highest potential possible applied across the shortest possible capillary length) favor high resolution: we use 30 kV and ~31 cm capillaries throughout. These choices represent the upper and lower limits, respectively, in commercially available instrumentation. The choice of a short capillary appears to be counterintuitive to the popular operating principle in chromatography where increasing the column length provides greater resolution; increasing the length of the capillary in CE may predict improved resolution, but, the concomitant decrease in the electric field compensates for this effect, providing no real net gain and instead lengthening the time before the analytes are detected. As such, the use of a longer capillary also results in increased diffusional band broadening, as shown in the formula for the Gaussian bell-shaped curve with the spatial variance  $\sigma_x$  (eq 2).<sup>24</sup> Contribution to band broadening resulting from diffusion is dependent on the diffusion coefficient ( $D$ ) of the analyte and the residence time in the capillary prior to detection ( $t$ , also known as the detection time). Because Joule heating is a concern under high field strengths, it is paramount that BGEs with the lowest possible conductivity are chosen. Although the use of sodium hydroxide as the titrant is commonly reported in the literature, we chose to use lithium hydroxide instead. Lithium borate buffers exhibit ~15% less conductivity than sodium borate buffers.

$$\sigma_x^2 = 2Dt \quad (2)$$

Figure 2 shows the traces obtained from CE analysis of a second-generation triazine dendrimer, a generation 1.5 DAB-PAMAM-C dendrimer, and a second-generation DAB-PAMAM-S dendrimer. These analytes were chosen because of the similarity in the number of terminal carboxylic acid groups. (See Table 1 for details.) An initial examination of the traces shows a single broad peak for the triazine dendrimer in contrast with multiple narrow peaks for the PAMAM dendrimers. Whereas it is clear that the PAMAM constructs exist as

a mixture of materials, the broadening observed for the triazine dendrimer could be attributed to a lack of resolution of a mixture of compounds or, at the other extreme, the sole result of diffusional broadening resulting from the longer time the analyte band remained in the capillary. Some insight is afforded by comparing time-corrected line widths. The width of a peak observed in CE at half-height ( $W_{1/2}$ ) is given by eq 3<sup>24</sup>

$$W_{1/2}=2.354\sigma \quad (3)$$

Combining eq 2 and eq 3 yields a direct correlation between  $W_{1/2}$  and  $t$  (eq 4)<sup>24</sup>

$$W_{1/2}=2.354(2Dt)^{1/2} \quad (4)$$

By assuming an identical diffusion coefficient for the PAMAM and the triazine dendrimers, a correlation can be derived for the widths of the peaks of the different dendrimer sets and the corresponding time the peaks were detected (eq 5).<sup>24</sup> Quantitative assessment indicates that the apparent wider peak for the triazine dendrimer is justified by accounting for the additional diffusion as a result of a longer detection time;  $W_{1/2}$  for the triazine dendrimer peak at ~3.3 min. should be, and is, ~1.6 times wider than the  $W_{1/2}$  for the PAMAM peak detected at ~1.2 min

$$W_{1/2,\text{triazine}}/W_{1/2,\text{PAMAM}}=t_{\text{triazine}}^{1/2}/t_{\text{PAMAM}}^{1/2} \quad (5)$$

Whereas the difference in dispersity in these materials is evident, these preliminary analyses provide additional clues with regard to the materials. Because of slight variations in the eof that drives the analytes in a direction opposite to their electro-phoretic migration, comparing the observed migration times is not valuable: the triazine dendrimer is not 1.6 times slower than the fastest component in the PAMAM series. However, an accurate assessment of migration velocities can be obtained by comparing the corresponding effective mobility values calculated from the migration times for the corresponding dendrimer peaks. The mobility value for the second-generation triazine dendrimer (having a maximum of 12 negative charges) is greater than those for the fastest component of the two PAMAM dendrimers, by ~10–20%, indicating that either the hydrodynamic radii for the corresponding PAMAM dendrimers is significantly larger than that of the triazine dendrimer or, in the case where the hydrodynamic radii are comparable, the partially protonated state of the amines in the PAMAM dendrimers at pH 9.1 diminishes the effective negative charge of the carboxylate groups to a value less than -12.

**$\beta$ , Effect of Electroosmotic Flow on Resolution**—Equation 1 emphasizes the influence of the transport coefficient ( $\beta$ ) on resolution, accounting for the amount of time the analytes spend under the applied electric field by means of the eof. The highest resolution between two charged analytes can be obtained when  $\beta = -1$  because it is under these conditions that the less mobile component is migrating with the same velocity and in the opposite direction as the eof. Efficient control of eof can be achieved by a variety of means, for example, by modifying the capillary surface using dynamic or permanent coating procedures, by changing the pH or the ionic strength of the BGE, and by the use of organic solvents. Figure 3 shows the effect of  $\beta$  on the separation of the second-generation triazine dendrimer and two PAMAM dendrimers with a similar number of carboxylate groups. Superficially, as  $\beta$  approaches -1, the traces appear to become worse as the signals become much wider. “Worse” is a result of band broadening due to the longer run times that are required for detection of all of the analyte components combined with the effect of lower

linear velocity with which the analytes travel past the detector. However, closer inspection reveals, in most cases, a successful baseline resolution of observed peaks, which have been numbered arbitrarily in Figure 3 to facilitate inspection. The signal-to-noise ratio decreases because of the constant diffusion of the analytes. Converting the scale from time values to effective mobility values helps us to better visualize signals (Figure 4) and aides the tracking of peaks because unlike detection time, electro-phoretic effective mobility values do not change with changes in eof.

The manipulation of  $\beta$  significantly improves resolution for the triazine dendrimers. Minor impurities indicated with “\*” and integrating to ~3% time-corrected peak area with respect to the major component are resolved. These species display less negative charge than the major species (assuming similar hydrodynamic radii), which suggests that these could possibly belong to incompletely succinylated triazine dendrimers. Mass spectrometry is consistent with this observation. One or two minor lines attributed to dendrimers lacking a succinic acid group as well as loss of water attributed to imide formation can be observed in some batches. (See the Supporting Information for representative spectra.) For generation 1.5 DAB-PAMAM-C and second-generation DAB-PAMAM-S dendrimers, marked improvements in resolution were also observed. However, only slight improvements were observed in the next higher generation dendrimers of the respective sets. The electropherograms obtained for the PAMAM dendrimers show several species with very similar effective mobility values: some baseline-resolved species differ by only as much as  $0.3 \times 10^{-5} \text{ cm}^2 \text{ V}^{-1} \text{ s}^{-1}$ , whereas “shoulders” with more similar mobility values are also observed. These indicate that the commercial PAMAM dendrimers analyzed in this study are highly disperse mixtures of species with very similar charge-to-size ratios. Without identifying which of the peaks belongs to the dendrimer as structurally described on the label, it is difficult to infer clues to structural information for the remaining signals. Efforts to describe the observed signals further are currently ongoing.

**$\alpha$ , Ionic Strength versus Buffering Capacity**—Further resolution of components in the individual PAMAM dendrimer mixtures was attempted by affecting the mobility ratio ( $\alpha$ ) through manipulation of parameters that influence the effective mobilities of the dendrimer species. Mobility values can vary strongly with ionic strength ( $I$ ). An empirical expression has been reported<sup>25</sup> for the actual mobility of fully dissociated organic anions with charge numbers ( $z_i$ ) between two and six in the ionic strength range of 1–100 mM shown below as eq 6

$$\mu/\mu_0 = \exp[-0.77(z_i I)^{1/2}] \quad (6)$$

where  $\mu$  is the actual mobility of the analyte and  $\mu_0$  is the mobility of the analyte at infinite dilution. Although a similar equation applicable to organic anions with higher charge numbers is not available in the literature, the general trend still holds true: increasing  $I$  decreases the actual mobility of the analytes. The influence of  $I$  on the actual mobility of the analyte increases with increasing charge number of the analyte. For example, in a mixture of components with a different number of carboxylic acids per component, the mobility of the component with the lowest number of carboxylic acids will decrease to a certain extent, but the mobility of the component with the highest number of carboxylic acids will decrease to a much greater extent. This difference causes a loss in resolution. Depending on the values of  $I$  and  $z_i$ , the two peaks can ultimately comigrate. To enhance the resolution of components in PAMAM dendrimer mixtures, BGEs with the lowest possible  $I$  are ideal. However, because sufficient buffering capacity is also desired, an optimum BGE must provide sufficient buffering capacity without the unnecessary (and detrimental) excess in ionic strength.



Therefore, analysis was done using borate buffer BGEs of different ionic strengths but the same pH values. (As mentioned earlier, for borate buffers, this is only true at pH 9.1).

Figure 5 shows the CE traces obtained for the second-generation DAB-PAMAM-S dendrimer and the second-generation triazine dendrimer, obtained using BGEs of different  $I$ . First, the trace for the DAB-PAMAM-S dendrimer obtained using the 20 mM borate buffer ( $I = 10$  mM) shows one major component, along with a few minor impurities, indicating high purity. However, the trace obtained using the 100 mM borate buffer ( $I = 50$  mM) shows the previously identified single component as a mixture of species with very close mobility values, suggesting that the 20 mM buffer did not provide the necessary buffering capacity in the previous run to show adequate resolution of components. Further increase in buffer concentration appears to decrease resolution, perhaps because of the effect of increasing ionic strength. Traces obtained for the second-generation triazine dendrimer under identical conditions further support the notion that a 100 mM borate buffer provided sufficient buffering capacity. However, unlike the peak for the DAB-PAMAM-S dendrimer, which resolved into multiple peaks, a single peak was consistently observed for the triazine dendrimer.

The measured effective mobility for the main component in the third-generation DAB-PAMAM-S dendrimer (electropherograms not shown) decreases by  $\sim 10\%$  (from  $-39.8 \times 10^{-5}$  to  $-36.1 \times 10^{-5}$   $\text{cm}^2/\text{V s}^{-1}$ ) when the  $I$  is increased from 10 to 50 mM. Increasing  $I$  from 50 to 100 mM decreases the mobility of the major component by  $<1\%$  (which is within the range of error in the measurement of mobility values). When compared with values calculated using eq 6, the inability to predict these mobility values accurately indicates that the effective negative charge on these dendrimers at pH 9.1 is greater than six. Unfortunately, changing ionic strength did not lead to an improvement in the resolution of higher-generation dendrimers. (Data not shown.)

**$\alpha$  as a Function of pH**—Just as  $\alpha$  can be optimized by identifying the appropriate  $I$  of the BGE to be used (because  $I$  affects effective mobility,  $\mu_{\text{eff}}$ ), for weak electrolytes,  $\mu_{\text{eff}}$  can also be altered by changing the pH of the BGE. The effective mobility of a weak electrolyte is given by the following equation

$$\mu_{\text{eff}} = \mu_i X_i \quad (7)$$

where  $\mu_i$  is the actual ionic mobility and  $X_i$  is the fraction of dissociation of the weak electrolyte. This equation can be extended to polyelectrolytes.<sup>26</sup> For purposes of analysis by CE, the value for  $X_i$  depends on the  $\text{p}K_a$  of the weak electrolyte, the temperature at which analysis is performed, and the pH and ionic strength of the BGE.

To probe the effect of pH on resolution of dendrimers, the three sets of dendrimers were analyzed using two phosphate/ lithium buffers: 20 mM buffer (pH 6.9;  $I = 40$  mM) and 50 mM buffer (pH 6.9;  $I = 100$  mM). Once again, the use of lithium hydroxide instead of sodium hydroxide here results in BGEs with  $\sim 17\%$  less conductivity. Comparison of peak resolution (as done previously with borate buffers) led to the conclusion that the 20 mM buffer did not provide adequate buffering capacity (data not shown), whereas the 50 mM buffer was sufficient.

Figure 6 shows the comparison of traces recorded using pH 9.1 (borate/lithium) and 6.9 (phosphate/lithium) BGEs for a series of PAMAM and triazine dendrimers. Enhanced baseline resolution for components of the second-generation DAB-PAMAM-S dendrimer mixture was achieved at pH 6.9 under favorable  $\beta$  conditions. The major component shown as a single peak in the third-generation DAB-PAMAM-S in the borate buffer also begins to

separate out into a broad signal with evidence of underlying peaks with similar mobility values. Although no visual enhancement of resolution was observed for the higher generations of PAMAM dendrimers analyzed, quantitative analysis of the range of mobility values included within the major signal indicated an enhanced mobility ratio ( $\alpha$ ; e.g.,  $\Delta\mu$  for generation 4.5 DAB-PAMAM-C analyzed using the borate buffer was  $3.7 \times 10^{-5} \text{ cm}^2 \text{ V}^{-1} \text{ s}^{-1}$ , whereas using the phosphate buffer  $\Delta\mu = 8.5 \times 10^{-5} \text{ cm}^2 \text{ V}^{-1} \text{ s}^{-1}$ ). Additional information regarding the  $\text{p}K_a$  values of the carboxylic acid groups can be inferred from these observations.

Because  $\alpha$ , the mobility ratio, or the selectivity, is defined as the ratio of the mobilities of the two analytes being separated (analytes 1 and 2, where 2 is the slower analyte)

$$\alpha = \mu_1 / \mu_2 \quad (8)$$

and mobility is proportional to the charge-to-size ratio of the analyte,  $\alpha$  can be related to charge state and eq 8 can be transformed into the following expression, where the symbol  $\leftrightarrow$  indicates proportionality

$$\alpha \leftrightarrow (z_1/r_1)/(z_2/r_2)$$

Assuming that the hydrodynamic radii of the two analytes are comparable, just as in the case of two dendrimer molecules of the same generation and different in the number of succinic acid groups, this expression can directly relate  $\alpha$  to  $z$

$$\alpha \leftrightarrow z_1/z_2$$

For the PAMAM dendrimers, the net effective charge of the dendrimer molecule at a given pH will be

$$z_1 = z_1^+ + z_1^- \quad (9)$$

where  $z_1^+$  and  $z_1^-$  are the effective cationic charge and effective anionic charge on the dendrimer molecule, respectively.

When a pH 6.9 BGE is used (instead of the pH 9.1 borate/lithium buffer), a decrease in the effective mobility is observed resulting from an increase in the degree of protonation, as is expected for both PAMAM and triazine dendrimers. In addition, however, an unexpected increase in the mobility spread unique to the higher-generation PAMAM dendrimers is observed. A series of initial calculations for two hypothetical molecules, with  $\text{p}K_a$  values for amines and carboxylic acids estimated on the basis of the works of Huang et al.,<sup>10</sup> Zhang et al.,<sup>27</sup> and Castagnola et al.,<sup>28</sup> suggests that the observed increase in the mobility spread is caused by a combined effect of differences in both the effective positive and effective negative charges on the two molecules. Structurally, this would translate to the fastest and the slowest molecule within the observed band having not only a different number of carboxylic acids, as earlier anticipated, but also a different number of aliphatic amines, possibly with correspondingly different  $\text{p}K_a$  values. A detailed investigation of this possibility requires a rigorous assessment of heterogeneity and purity of the cationic precursors to these anionic dendrimers using strategies similar to what has been done in this work.

The behavior of the triazine dendrimers however, is consistent with higher purity materials. Minor impurities, with less-negative effective mobility values compared with the major component, were still found to be reasonably resolved in the trace for second-generation triazine dendrimer (having 12 negative charges). The time-corrected peak areas for these minor impurities integrated to a similar corrected percent peak area, as previously observed using the borate buffer. New trace level impurities with less-negative mobilities than the major component were observed using the phosphate buffers in the analysis of third-generation triazine dendrimer (having 24 negative charges). In addition, the broadness of the peaks suggest the presence of species with differences in charge-to-size ratio that are smaller than those expected from the presence of incompletely succinylated derivatives. This hints toward our long-standing suspicion that triazine dendrimers tend to aggregate in aqueous solutions. Similarly, second-generation and generation 1.5 PAMAM dendrimers (having 16 negative charges) and third-generation and generation 2.5 dendrimers (having 32 negative charges) appear to be resolved, whereas higher generations (having 64 and 128 negative charges) escape resolution. Overall, these studies also set bounds on our confidence in employing CE to resolve impurities in dendrimer systems that vary slightly in their charge state.

To further evaluate the conditions developed and the hypothesis of high purity, we performed substoichiometric succinylations of the generation 2 triazine dendrimer while monitoring these reactions with CE and MALDI-MS. Figure 7 shows the results. The broad traces observed for traces A–C (0.25 to 0.75 equiv of succinic anhydride) are markedly different than the almost completely succinylated dendrimer in trace D. Analysis of these by MALDI-MS confirms a distribution of peaks. The shoulder on the left edge of D suggests the presence of impurities. The MALDI-MS trace shows a tiny line above noise corresponding to one succinate missing. Overall, we infer that the synthesized triazine dendrimers reported here have purities of ~95%.

## Conclusions

CE shows broad utility during the characterization of low-generation anionic dendrimers that might be extended for use in the assessment of purity and the assessment of batch-to-batch reproducibility during synthesis. The conversion of the time scale in obtained electropherograms to an effective mobility scale allows for a more accurate evaluation of data. Resolution obtained from CE analysis is dependent on several interdependent operational parameters. Whereas the original goals of this study were to better assess the purity of triazine dendrimers, what has emerged is a stepwise protocol for optimizing resolution in our system. Moreover, the protocol and parameters adopted may find broader utility: this method is recommended for the assessment of dendrimeric systems. The methods used can be readily employed; the success achieved with unmodified capillaries does not require the exploration of covalently coated capillaries.

Although results from CE analysis of anionic commercially available PAMAM dendrimers could support the notion of heterogeneity due to aggregate formation, we favor a simpler explanation. We infer that these dendrimers are mixtures with highly complex molecular diversities, increasing with generation number. In contrast, anionic triazine dendrimers more closely approach single-molecule systems. To settle the argument of aggregation versus compositional heterogeneity in PAMAM systems, further study on the structural identification of the various peaks detected using CE is needed and is currently ongoing. Lastly, the variation in the peak patterns and effective mobility spread under different BGE conditions observed in the analysis of PAMAM dendrimers using CE can pose difficulties in physicochemical characterization studies where accurate determination of effective mobility values as a function of the parameter under study is crucial. Such investigations should,

however, find success when applied to the characterization of triazine dendrimers. These studies raise additional questions as well. We are curious about how the effective mobility values of anionic dendrimers with charge numbers greater than six change as a function of the ionic strength of the BGE. The answer is important and could translate to proteins and DNA analysis by CE. We also wonder how the effective mobility changes as a function of pH; that is, what are the dissociation constants for the weak electrolyte functional groups on these dendrimers (for both amines and carboxylic acids). Answers to both questions could help make the method optimization process more efficient. In conclusion, we remain optimistic that these triazine dendrimers could ultimately be adopted into materials with applications wherein the demands of purity can be satisfied.

## Acknowledgments

This work was supported by the NIH (EES R01 GM64560) and (SS 5U01A1095351-02).

## References and Notes

1. Khandare J, Kohle P, Pillai O, Kannan S, Lieh-Lai M, Kannan RM. *Bioconjugate Chem* 2005;16:330–337.
2. Myc A, Majoros I, Thomas TP, Baker JR Jr. *Biomacromolecules* 2007;8:13–18. [PubMed: 17206782]
3. Islam MT, Majoros I, Baker JR Jr. *J. Chromatogr., B: Anal. Technol. Biomed. Life Sci* 2005;822:21–26.
4. Wu G, Barth RF, Yang W, Kawabata S, Zhang L, Green-Church K. *Mol. Cancer Ther* 2006;5:52–59. [PubMed: 16432162]
5. Caminade A-M, Laurent R, Majoral J-P. *Adv. Drug Deliv Rev* 2005;57:2130–2146.
6. Shi X, Wojciech L, Islam MT, Muniz MC, Balogh LP, Baker JR Jr. *Colloids Surf., A* 2006;272:139–150.
7. Chouai A, Simanek EE. *J. Org. Chem* 2008;73:2357–2366. [PubMed: 18307354]
8. Cason CA, Oehrle SA, Fabre TA, Girten CD, Walters KA, Tomalia DA, Haik KL, Bullen HA. *J. Nanomater* 2008;7:456082.
9. Cottet H, Simo C, Vayaboury W, Cifuentes A. *J. Chromatogr., A* 2005;1068:59–73. [PubMed: 15844543]
10. Huang QR, Dublin PL, Moorefield CN, Newkome GR. *J. Phys. Chem. B* 2000;104:898–904.
11. Seyrek E, Dublin PL, Newkome GR. *J. Phys. Chem. B* 2004;108:10168–10171.
12. Shi X, Patri A, Wojciech L, Islam MT, Zhang C, Baker JR Jr, Balogh LP. *Electrophoresis* 2005;26:2960–2967. [PubMed: 16007703]
13. Brothers HM Jr, Piehler LT, Tomalia DA. *J. Chromatogr., A* 1998;814:233–246.
14. Desai A, Shi X, Baker JR Jr. *Electrophoresis* 2008;29:510–515. [PubMed: 18080252]
15. Crampton H, Hollink E, Perez L, Simanek EE. *New J. Chem* 2007;31:1283–1290.
16. Williams BA, Vigh G. *Anal. Chem* 1996;68:1174–1180.
17. Quintana A, Raczka E, Piehler L, Lee I, Myc A, Majoros I, Patri AK, Thomas T, Mule J, Baker JR Jr. *Pharm. Res* 2002;19:1310–1316. [PubMed: 12403067]
18. Uppuluri S, Swanson DR, Piehler LT, Li J, Hagnauer GL, Tomalia DA. *Adv. Mater* 2000;12:796–800.
19. Hollink E, Simanek EE. *Org. Lett* 2006;8:2293–2295. [PubMed: 16706509]
20. Gas B, Coufal P, Jaros M, Muzikar J, Jelinek I. *J. Chromatogr., A* 2001;905:269–279. [PubMed: 11206794]
21. Jaros M, Vcelakova K, Zuskova K, Gas B. *Electrophoresis* 2002;23:2667–2677. [PubMed: 12210171]
22. Āas, B. Group of Electromigration Separation Processes. <http://www.natur.cuni.cz/gas>
23. Rawjee YY, Vigh G. *Anal. Chem* 1994;66:619–627.

24. Kenndler, E. Theory of Capillary Zone Electrophoresis. In: Khaledi, M., editor. High-Performance Capillary Electrophoresis: Theory, Techniques, and Applications. Vol. Vol. 146. New York: John Wiley; 1998. p. 25-76.
25. Friedl W, Reijenga JC, Kenndler E. J. Chromatogr., A 1995;709:163–170.
26. Vcelakova K, Zuskova I, Kenndler E, Gas B. Electrophoresis 2004;25:309–317. [PubMed: 14743483]
27. Zhang H, Dublin PL, Kaplan J, Moorefield CN, Newkome GR. J. Phys. Chem. B 1997;101:3494–3497.
28. Castagnola M, Zuppi C, Rossetti DV, Vincenzoni F, Lupi A, Vitali A, Meucci E, Messina I. Electrophoresis 2002;23:1769–1778. [PubMed: 12116119]

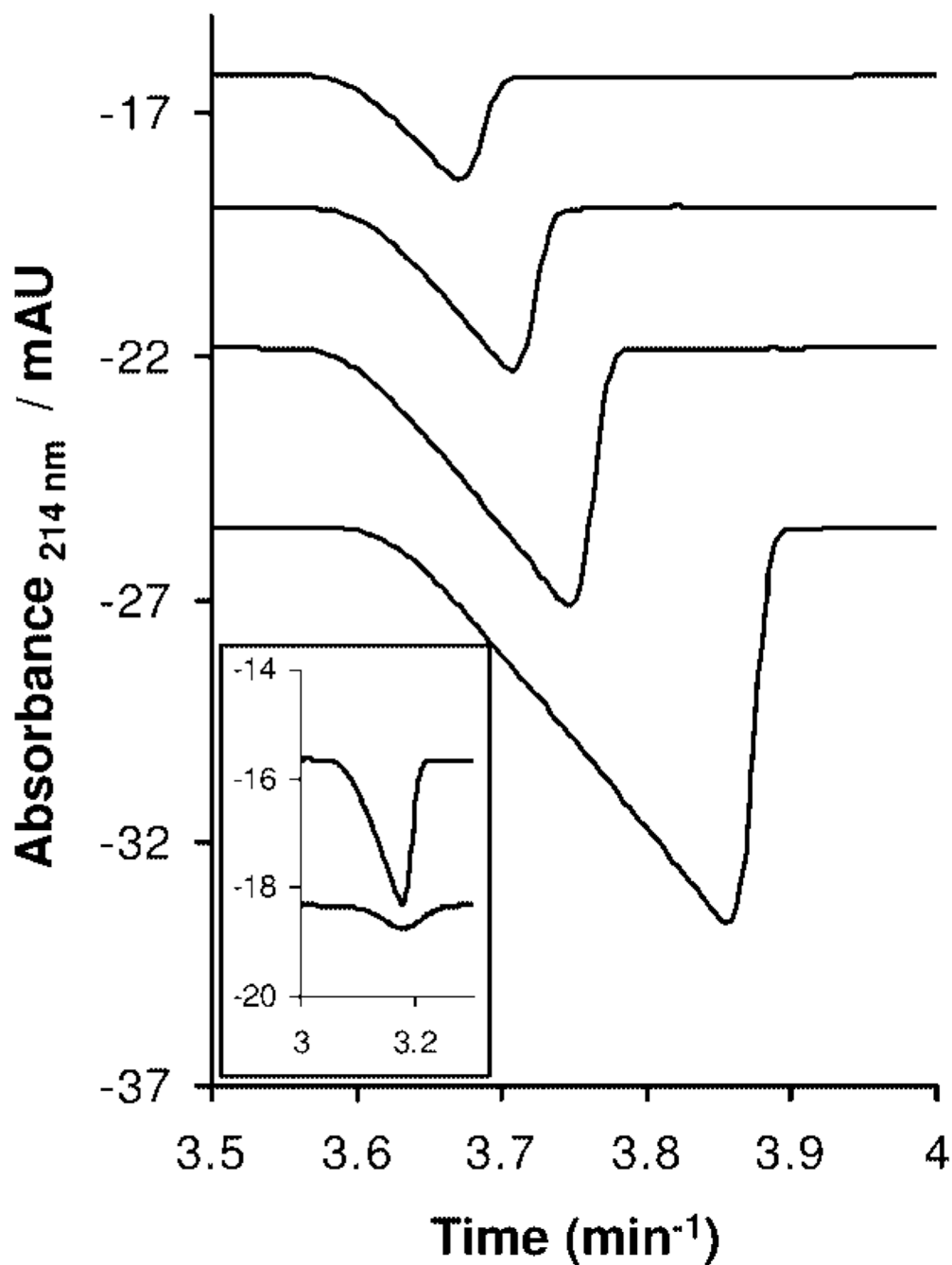


**Figure 1.** Traces for succinic acid calibration standards obtained using indirect-UV detection CE ( $R^2 = 0.999$ ; RSD = 3.48). Inset shows the CE traces for excess succinate in the triazine dendrimer reaction mixture after first and second purification cycles.

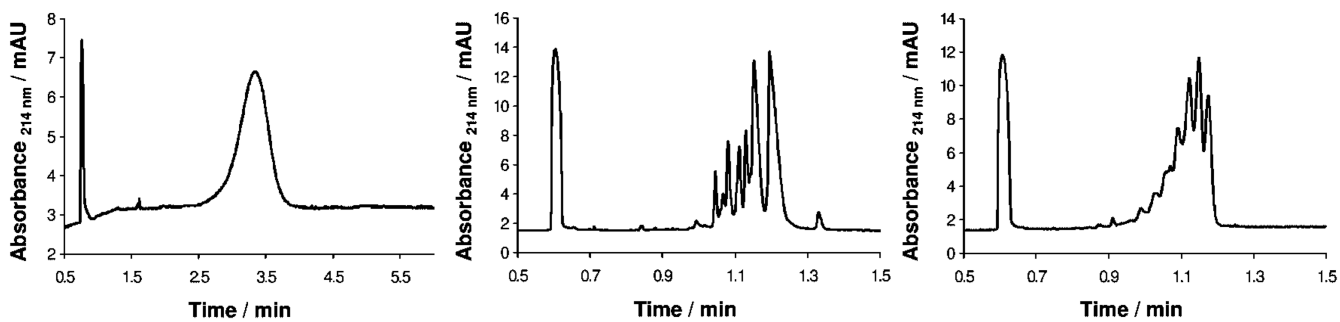


**Figure 2.** Electropherograms for second-generation triazine dendrimer (left), generation 1.5 DAB-PAMAM-C dendrimer (center), and second-generation DAB-PAMAM-S dendrimer (right). All runs were performed in positive-to-negative polarity (positively charged electrode at the injection end of the capillary).

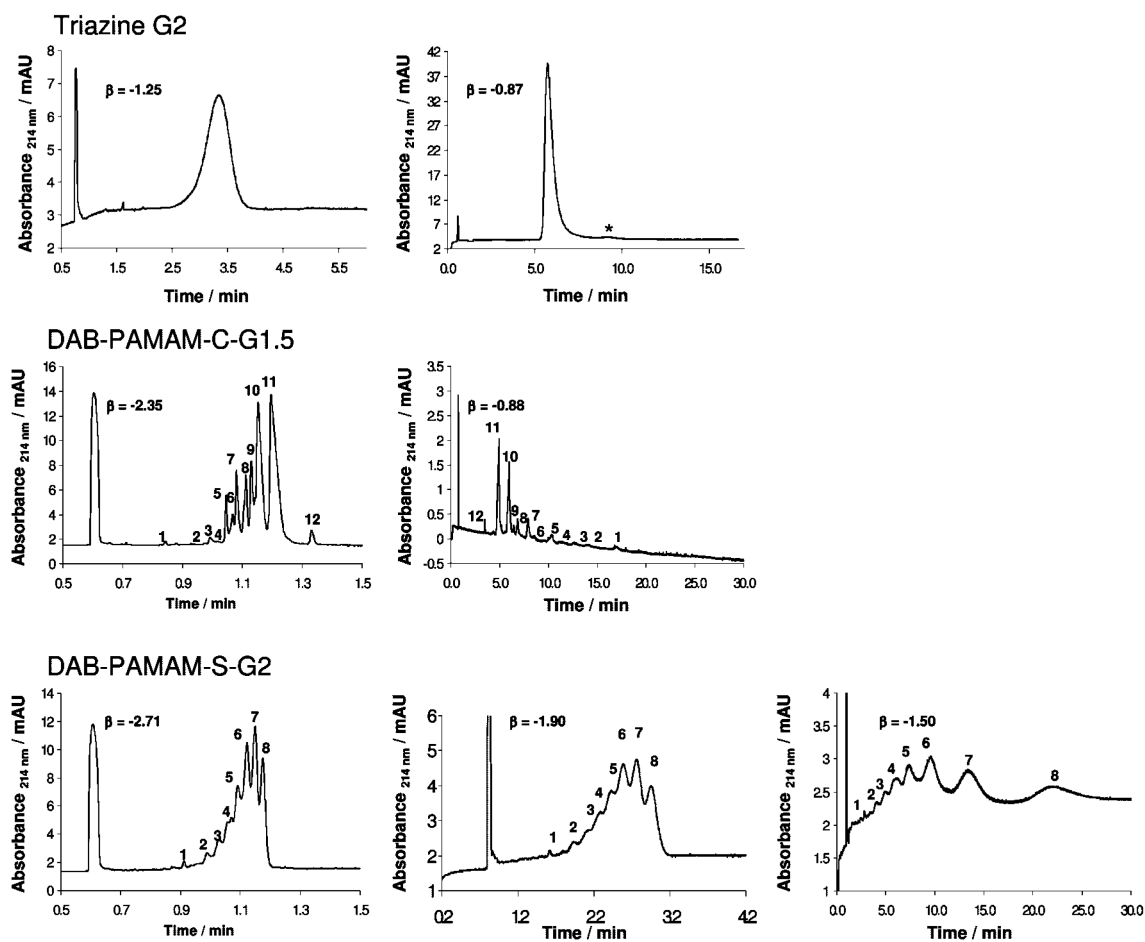


**Figure 3.** Electropherograms obtained for second-generation triazine dendrimer (top panel), generation 1.5 DAB-PAMAM-C (middle panel), and second-generation DAB-PAMAM-S (bottom panel) under different  $\beta$  values. The first peak in all traces is the neutral marker peak (DMSO). All runs were performed in positive-to-negative polarity, except for the traces with  $\beta$  values of  $-0.87$  and  $-0.88$  respectively, which were run in negative-to-positive polarity.



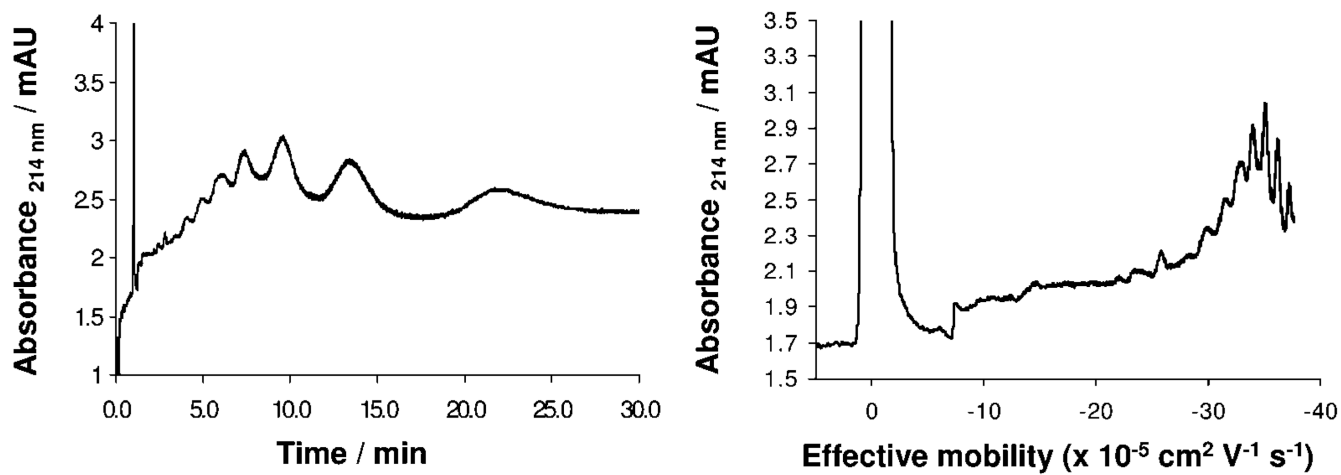


**Figure 4.** Electropherograms for second-generation DAB-PAMAM-S dendrimer on detection time (left) and effective mobility (right) scales. Trace with mobility scale was obtained using the Microsoft Excel software package.

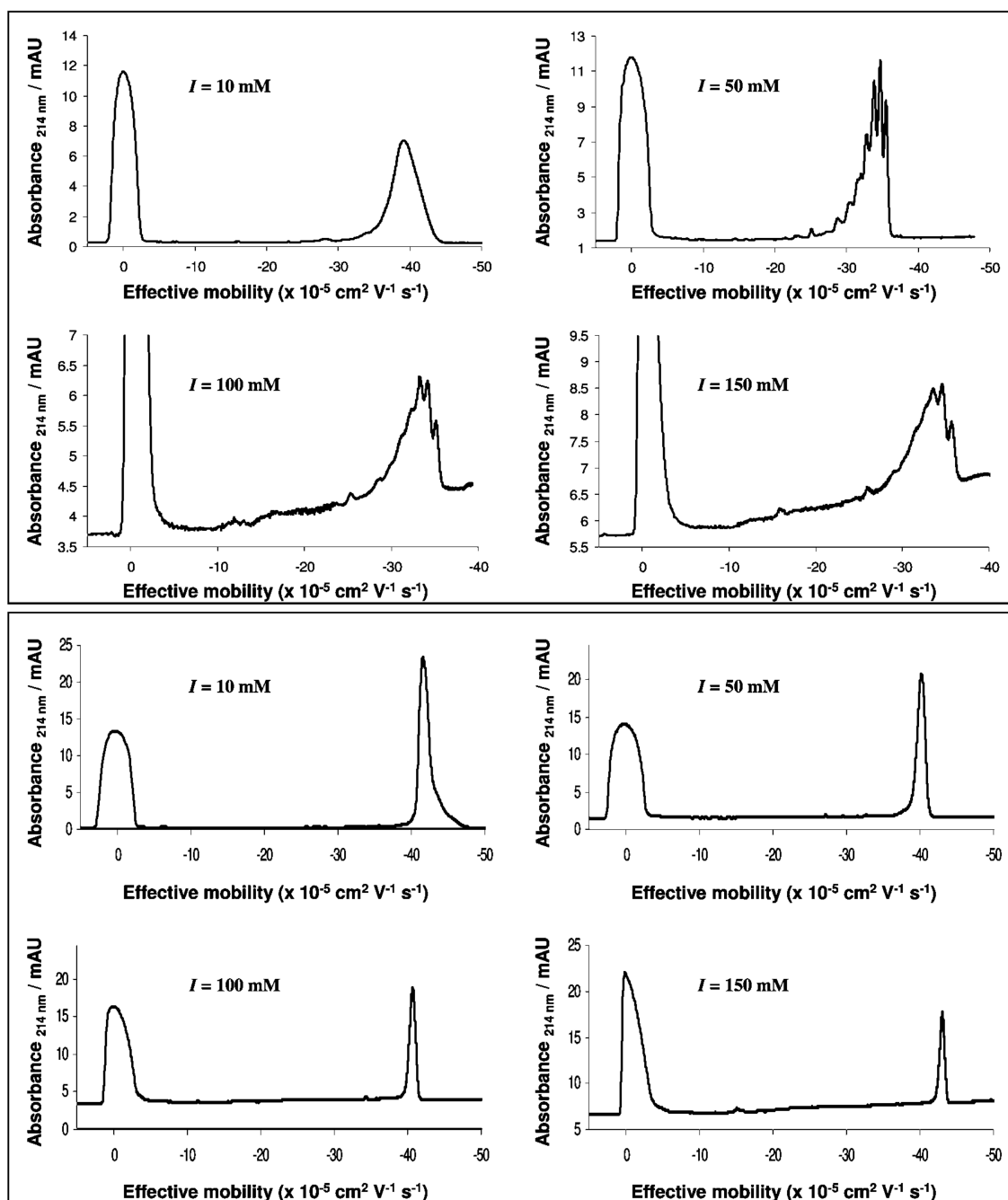


**Figure 5.** Electropherograms for the second-generation DAB-PAMAM-S dendrimer (top panel) and the second-generation triazine dendrimer (bottom panel) obtained using pH 9.1 borate/lithium buffers with different ionic strengths ( $I$ ), as shown in the respective traces.

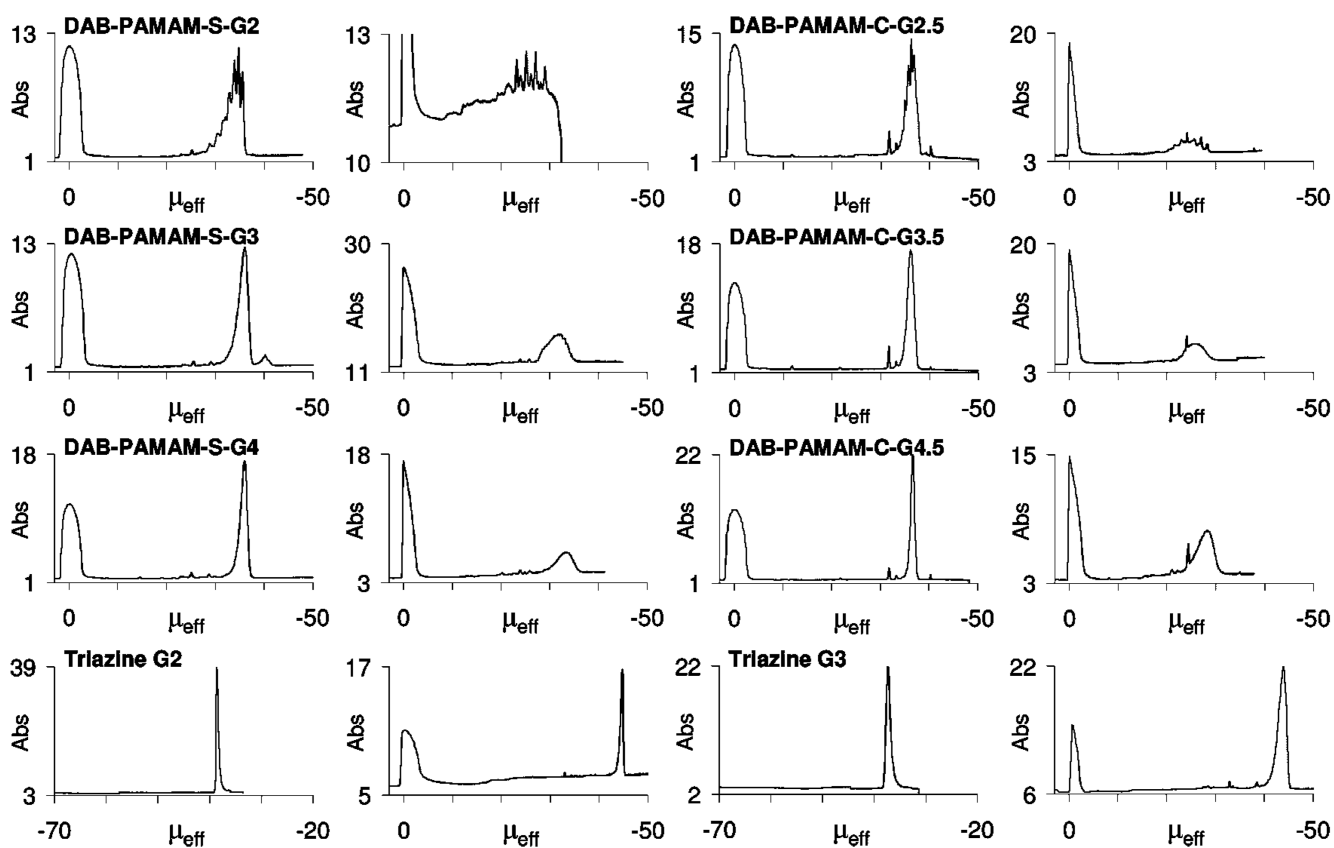


**Figure 6.**

Electropherograms for the three dendrimer classes obtained using pH 9.1 100 mM borate/lithium buffer (left) and using pH 6.9 50 mM phosphate/lithium buffer (right). All traces were obtained in positive-to-negative polarity, except traces for triazine dendrimers using borate buffer, which were obtained in negative-to-positive polarity. The absorbance scale (Abs) is in milli-absorbance units (mAU) recorded at a 214 nm detection wavelength. Effective mobility scale ( $\mu_{\text{eff}}$ ) is in “ $\times 10^{-5} \text{ cm}^2/\text{V} \cdot \text{s}$ ” units.

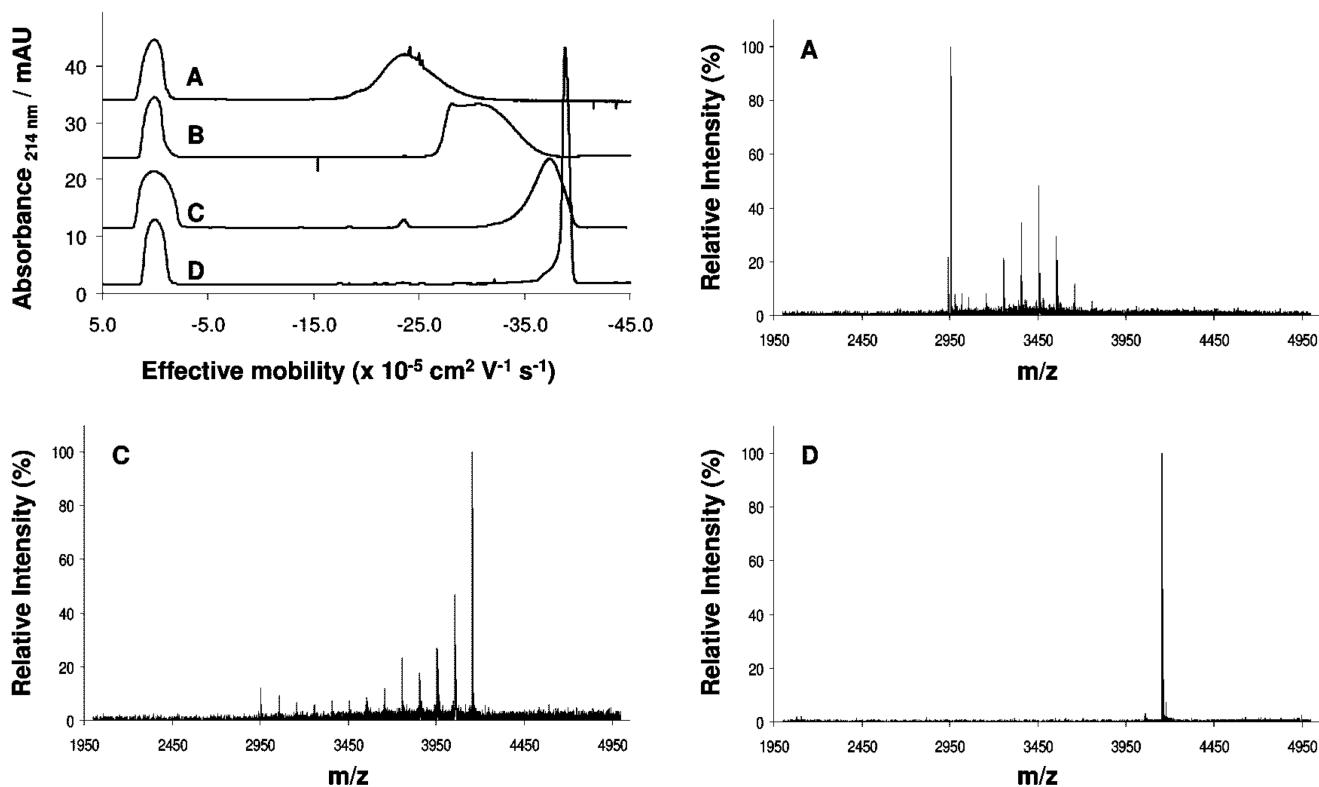
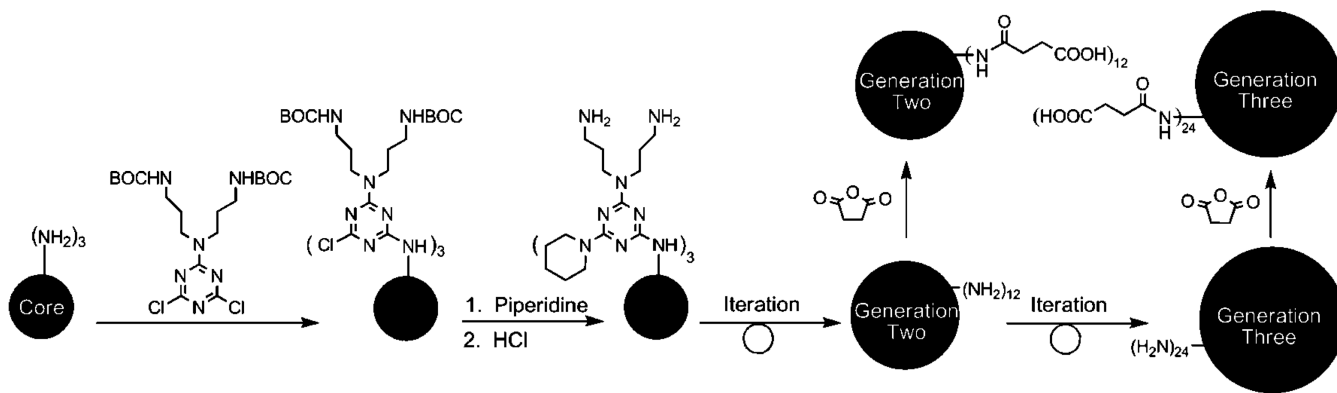


**Figure 7.**

CE traces (top left) and corresponding MALDI-TOF-MS spectra for samples obtained during the monitoring of the succinylation of the second-generation triazine dendrimer: *A* = 0.25 mol succinic anhydride/mol  $\text{NH}_2$ ; *B* = 0.5 mol succinic anhydride/mol  $\text{NH}_2$ ; *C* = 0.75 mol succinic anhydride/mol  $\text{NH}_2$ ; *D* = 1.0 mol succinic anhydride/mol  $\text{NH}_2$ .



**Scheme 1.**  
Synthesis of the Anionic Triazine Dendrimers

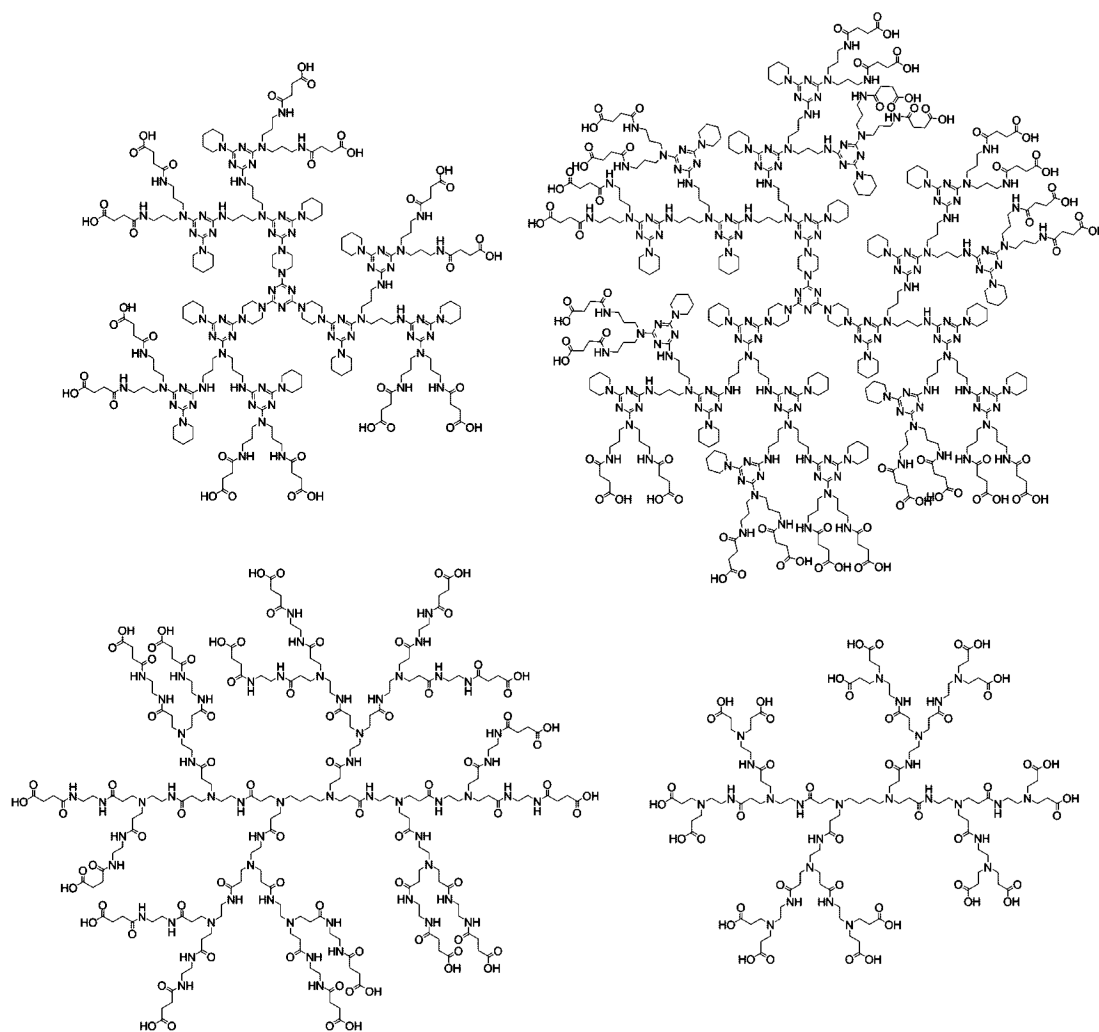


**Chart 1.**  
Structures for Second-Generation Triazine Dendrimer (Top Left), Third-Generation Triazine Dendrimer (Top Right), Second-Generation DAB-PAMAM-S Dendrimer (Bottom Left), and Generation 1.5 DAB-PAMAM-C Dendrimer (Bottom Right)

**Table 1**List of Dendrimers Evaluated in This Study and Their Corresponding Number of Carboxylic Acid Groups<sup>a</sup>

DAB-PAMAM-C	DAB-PAMAM-S	triazine
G1.5 16	G2 16	G2 12
G2.5 32	G3 32	G3 24
G3.5 64	G4 64	
G4.5 128	G5 128	

<sup>a</sup>In the case of the PAMAM dendrimers, the number of interior aliphatic amines is two less than the number of carboxylic acid groups. Triazines have no aliphatic amines. The number of carboxylic acid groups for PAMAM dendrimers is theoretical: structural defects can result in numbers less than the listed theoretical values.